RSC Advances

ROYAL SOCIETY OF CHEMISTRY

www.rsc.org/advances

A combined experimental and computational study of supramolecular assemblies in ternary copper(II) complexes with a tetradentate N_4 donor Schiff base and halides

Anik Bhattacharyya, Prasanta Kumar Bhaumik, Antonio Bauzá, Partha Pratim Jana, Antonio Frontera, Michael G. B. Drew, Shouvik Chattopadhyay

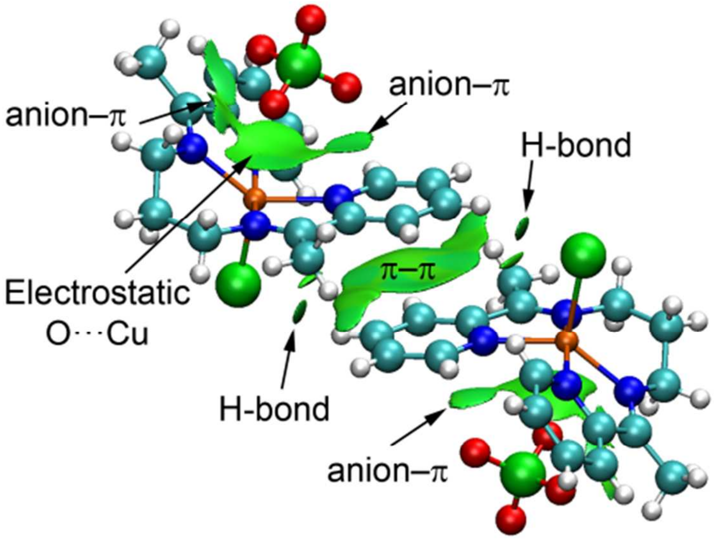

Three new copper(II) complexes, have been prepared from a tetradentate symmetrical Schiff base and characterized by elemental analysis, IR and UV–Vis spectroscopy and single-crystal X-ray diffraction studies. Density functional theory (DFT) calculations were employed to estimate the contribution of each interaction to the formation of the assembly using several theoretical models. The interplay between the anion–π and π–π interactions are also analyzed and a mutual reinforcement of both interactions is demonstrated.

RSC ADVANCES RSCPublishing

ARTICLE

Cite this: DOI: 10.1039/x0xx00000x

Received 00th January 2012,
Accepted 00th January 2012

DOI: 10.1039/x0xx00000x

www.rsc.org/

A combined experimental and computational study of supramolecular assemblies in ternary copper(II) complexes with a tetradentate N_4 donor Schiff base and halides

Anik Bhattacharyya[a], Prasanta Kumar Bhaumik[a], Antonio Bauzá[b], Partha Pratim Jana[c], Antonio Frontera[b,*] Michael G. B. Drew[d], Shouvik Chattopadhyay[a,*]

Three new copper(II) complexes, *[Cu(L)(Cl)]ClO₄* (**1**), *[Cu(L)(Br)]ClO₄* (**2**) and *[Cu(L)(I)]ClO₄* (**3**), have been prepared from a tetradentate symmetrical Schiff base, N,N'-bis-(1-pyridin-2-yl-ethylidene)-propane-1,3-diamine (L) and characterized by elemental analysis, IR and UV–Vis spectroscopy and single-crystal X-ray diffraction studies. Density functional theory (DFT) calculations were employed to estimate the contribution of each interaction to the formation of the assembly using several theoretical models. The interplay between the anion–π and π–π interactions are also analyzed and a mutual reinforcement of both interactions is demonstrated. The assignment of the contribution of each interaction and its mutual influence is certainly important to shed light into the delicate mechanism that governs the molecular recognition and crystal packing.

Introduction

The constructions of supramolecular networks with interesting non-covalent interactions are important binding forces in many areas of chemistry and biochemistry. In particular, the construction supramolecular assemblies is considered as an interesting research topic due to the new possibilities to prepare structures with different size and shape.[1] Understanding the formation of the assemblies through the variety of cooperative noncovalent interactions is crucial to gain knowledge in this field. Several well established noncovalent interactions such as hydrogen bonding,[2] π-stacking,[3] cation–π,[4] C–H/π[5] forces have been used to govern the organization of multi-component supramolecular assemblies. Moreover, other less established forces like lone-pair···π[6] and anion–π interactions[7] have open new possibilities in supramolecular recognition and have emerged as a new concept in anion-transport, anion-sensing and anion-recognition chemistry,[8] transmembrane anion transport[9] and catalysis.[10] In particular, the relevance of noncovalent anion–π interaction, which occurs between an electron-deficient aromatic system and an anion, has been evidenced in the gas phase,[11] in solution,[12] solid-state,[13] and broadly analyzed by means of theoretical[14] and experimental investigations.[15]

Chelating ligands have played a vital role in the progress of the coordination chemistry related to magnetism, molecular architectures, enzymatic reaction etc.[16] Amongst them, the increasing popularity of the Schiff bases is probably related with their facile synthesis and good properties like flexibility and complexation ability.[17] The synthesis of the symmetrical di-Schiff bases derived from 2-pyridyl carbonyl compounds has attracted a lot of attention as they could be used for the synthesis of metal complexes with exciting optical, magnetic and electrical properties.[18] They are also interesting for their potential abilities in biological modelling application,[19] e.g. to mimic the N_4 donor set of copper(II) in Cu_2Zn_2 superoxide dismutase (Cu_2Zn_2SOD).[20] A tetradentate symmetrical di-Schiff base ligand, N,N'-bis-(1-pyridin-2-yl-ethylidene)-propane-1,3-diamine (L) is widely used by several groups to prepare a number of copper(II) complexes.[21] We have also used this ligand in our previous work to prepare some copper(II) complexes with pseudo-halides as co-ligands.[22] This ligand contains several π systems with the potential ability to establish different supramolecular assemblies based on interactions involving π-systems.

Keeping this in mind, we report herein the synthesis of three new copper(II) complexes with this N_4 donor tetradentate Schiff base and with halide co-ligands. We have examined the structural features in detail that reveal supramolecular extended networks generated through weak non-covalent forces. In addition to the synthesis and X-ray characterization of the complexes, we shed light to the formation mechanism of the assemblies by means of density functional theory (DFT) calculations, estimating the contribution of each interaction to the formation of the assembly using several theoretical models. We also analyze the interplay between the anion–π and π–π interactions and we demonstrate a mutual reinforcement of both interactions. The assignment of the contribution of each interaction and its mutual influence is certainly important to shed light into the delicate mechanism that governs the molecular recognition and crystal packing.

Experimental

All chemicals were of AR grade and were used as purchased from Sigma-Aldrich without further purification.
Caution!!! Although no problems were encountered in this work, perchlorate salts containing organic ligands are potentially explosive. Only a small amount of the material should be prepared and they should be handled with care.

Synthesis of the ligand, L [N,N′-bis-(1-pyridin-2-yl-ethylidene)-propane-1,3-diamine]

The Schiff base ligand (L) was prepared by condensation of 1,3-diaminopropane (5 mmol, 0.42 cm^3) and 2-acetylpyridine (10 mmol, 1.2 cm^3) in methanol (25 cm^3) under reflux for 3h. The ligand was not isolated and the yellow coloured methanol solution was used directly for the synthesis of complexes.

Synthesis of [Cu(L)(Cl)]ClO$_4$ (1)

A methanol solution of copper(II) perchlorate (5 mmol, 1.85 g) was added into the methanol solution of the ligand (L) and refluxed for 1 h. A bright blue crystalline complex, *[CuL(ClO$_4$)$_2$],* was separated out on cooling and collected by filtration. A methanol solution (10 cm^3) of potassium chloride (1 mmol, 0.075 g) was added into the methanol solution of *[CuL(ClO$_4$)$_2$]* (1 mmol, 0.542 g). The mixture was stirred for 1h. Deep-green single crystals**,** suitable for X-ray diffraction, were obtained on slow evaporation of the methanol solution in open atmosphere.
Yield: 0.365 g (76%), Anal. Calc. for $C_{17}H_{20}Cl_2CuN_4O_4$ (FW 478.82): C, 42.64; H, 4.21; N, 11.70. Found: C, 42.70; H, 4.20; N, 11.65 %. IR (KBr, cm^{-1}) 1620 ($\nu_{C=N}$), 1088 (ν_{ClO4}); UV-Vis, λ_{max} (nm) [ε_{max}(dm^3 mol^{-1} cm^{-1})] (acetonitrile) 219 (2.775×10^4), 277 (1.255×10^4), 775 (229). Magnetic moment: 1.72 μ_B.

Synthesis of [Cu(L)(Br)]ClO$_4$ (2)

Complex **2** was prepared in a similar method as that of complex **1** except that potassium bromide (1 mmol, 0.119 g) was added instead of potassium chloride. X-ray quality single crystals were grown from acetonitrile solution.
Yield: 0.42 g (80%), Anal. Calc. for $C_{17}H_{20}BrClCuN_4O_4$ (FW 523.77): C, 39.02; H.3.85; N, 10.71; Found: C, 39.10; H, 3.80; N, 10.69%. IR (KBr, cm^{-1}) 1620 ($\nu_{C=N}$), 1085 (ν_{ClO4}); UV-Vis, λ_{max} (nm) [ε_{max}(dm^3 mol^{-1} cm^{-1})] (acetonitrile) 221 (3.2×10^4), 279 (1.295×10^4), 788 (336). Magnetic moment: 1.71 μ_B.

Synthesis of [Cu(L)(I)]ClO$_4$ (3)

Complex **3** was also prepared in a similar method as that of complex **1** except that potassium iodide (1 mmol, 0.166 g) was used instead of potassium chloride. X-ray quality, deep green single crystals were grown from DMSO solution.

Yield: 0.48 g (84%). Anal. Calc. (%) for $C_{17}H_{20}ClCuIN_4O_4$ (FW 570.27): C, 35.80; H, 3.53; N, 9.82. Found: C, 35.85; H, 3.50; N, 9.79.IR (KBr, cm^{-1}): 1593 ($\nu_{C=N}$), 1080 (ν_{ClO4}); UV-Vis, λ_{max} (nm) [ε_{max}, (dm^{3}mol^{-1}cm^{-1})] (acetonitrile) 242 (1.6839×10^4), 277 (1.002×10^4), 340 (2657), 820 (356). Magnetic moment: 1.72 μ_B.

Physical measurements

Elemental analysis (carbon, hydrogen and nitrogen) was performed using a PerkinElmer 240C elemental analyzer. IR spectra in KBr (4500–500 cm^{-1}) were recorded using a PerkinElmer FT-IR spectrometer Spectrum Two. Electronic spectra in acetonitrile (1200–200 nm) were recorded in JASCO V-630 Spectrophotometer. Fluorescence spectra were obtained on Shimadzu RF-5301PC spectrofluorophotometer at room temperature. The magnetic susceptibility measurements were done with an EG and PAR vibrating sample magnetometer, model 155 at room temperature (300 K) in 5000 G magnetic field and diamagnetic corrections were done using Pascal's constants.[23] Effective magnetic moments were calculated using the formula $\mu_{eff} = 2.828(\chi_M T)^{1/2}$, where χ_M is the corrected molar susceptibility. The instrument was calibrated using metallic nickel. Powder X-ray diffraction was performed on a Bruker D8 instrument with Cu-Kα radiation. In this process, the complexes were ground in a mortar pestle to prepare fine powders. The powders were then dispersed with alcohol onto a zero background holder (ZBH). The alcohol was allowed to evaporate to provide a nice, even coating of powder adhered to the sample holder.

X-ray Crystallography

Suitable crystals were picked, mounted on a glass fiber and diffraction intensities were measured with an Oxford Diffraction XCalibur, Eos equipped with Mo-Kα radiation (λ =0.71073 Å, 50 kV, 40 mA) at an ambient temperature (293 K). Data collection and reduction was performed with the Oxford diffraction Crysalis system. The structures of complexes were solved by direct methods and refined by full-matrix least squares on F^2, using the SHELX-97 package. Non-hydrogen atoms were refined anisotropically. The hydrogen atoms were placed in their geometrically idealized positions and constrained to ride on their parent atoms. Programs used: SHELXL-97,[24] PLATON,[25] DIAMOND,[26] ORTEP[27] and MERCURY.[28] Significant crystallographic data are summarized in Table 1. Selected bond lengths and bond angles are gathered in Table 2.

Computational methods

Table 1: Crystallographic data for complexes **1**-**3**.

	1	**2**	**3**
Formula	$C_{17}H_{20}Cl_2CuN_4O_4$	$C_{17}H_{20}BrClCuN_4O_4$	$C_{17}H_{20}IClCuN_4O_4$
Formula Weight	478.82	523.27	570.27
Crystal System	Triclinic	Triclinic	Triclinic
Space group	*P-1*	*P-1*	*P-1*
a (Å)	8.4513(4)	8.2691(17)	8.3319(6)
b (Å)	8.8335(4)	8.8985(8)	9.2183(6)
c (Å)	13.1616(6)	12.9934(15)	13.2704(11)
α (º)	92.630(4)	92.082(9)	91.819(6)
β (º)	94.799(4)	94.504(13)	94.151(6)
γ (º)	96.103(3)	96.468(12)	95.975(6)
Z	2	2	2
d_{cal} (g cm^{-3})	1.636	1.837	1.875
μ(mm^{-1})	1.430	3.440	2.772
F(000)	490	526	562
Total reflection	15689	8305	11938
Unique Reflections	4420	4255	4484
Observed data[I >2σ(I)]	3645	3273	3650
R_{int}	0.038	0.045	0.039
Goodness-of-fit	1.02	0.96	1.18
R1, *w*R2 (all data)	0.0592,0.1284	0.0595, 0.1054	0.0853,0.2839
R1, *w*R2 [I>2σ(I)]	0.0478,0.1218	0.0414, 0.0913	0.0664,0.2120

The energies of all complexes included in this study were computed at the BP86-D3/def2-TZVP level of theory. The geometries have been obtained from the crystallographic coordinates. The calculations have been performed by using the program TURBOMOLE (Version 6.5).[29] For the calculations we have used the BP86 functional with the latest available correction for dispersion (D3).[30]

We have used the NCI method[31] to study the double anion–π and π–π interactions observed in the X-ray structures. This method relies on two scalar fields to map local bonding properties: the electron density (ρ) and the reduced-density gradient (RDG, σ). It is able of mapping real-space regions where non-covalent interactions are important and is based exclusively on the electron density and its gradient. The information provided by NCI plots is essentially qualitative, i.e. which molecular regions interact. The color scheme is a red-blue scale with red for ρ^{+}_{cut} (repulsive) and blue for ρ^{-}_{cut} (attractive). Moreover, green and yellow isosurfaces correspond to weakly attractive and weakly repulsive interactions, respectively.

Hirshfeld Surface Analysis

Hirshfeld surfaces[32-34] and the associated 2D-fingerprint[35-37] plots were calculated using Crystal Explorer,[38] which accepted a structure input file in CIF format. Bond lengths to hydrogen atoms were set to standard values. For each point on the Hirshfeld isosurface, two distances d_e, the distance from the point to the nearest nucleus external to the surface and d_i, the distance to the nearest nucleus internal to the surface, were defined. The normalized contact distance (d_{norm}) based on d_e and d_i was given by

$$d_{norm} = \frac{(d_i - r_i^{vdw})}{r_i^{vwd}} + \frac{(d_e - r_e^{vdw})}{r_e^{vwd}}$$

where r_i^{vdW} and r_e^{vdW} were the van der Waals radii of the atoms. The value of d_{norm} was negative or positive depending on intermolecular contacts, being shorter or longer than the van der Waals separations. The parameter d_{norm} displayed a surface with a red-white-blue color scheme, where bright red spots highlighted shorter contacts, white areas represented contacts around the van der Waals separation, and blue regions were devoid of close contacts. For a given crystal structure and set of spherical atomic electron densities, the Hirshfeld surface was unique[39] and it was this property that suggested the possibility of gaining additional insight into the intermolecular interaction of molecular crystals.

Table 2: Selected bond lengths (Å) and bond angles (°).

	1 (X=Cl)	**2** (X=Br)	**3** (X=I)
Cu(1)–N(1)	2.089(3)	2.058(3)	2.067(6)
Cu(1)–N(2)	1.975(3)	1.950(3)	1.978(6)
Cu(1)–N(3)	2.015(3)	1.992(3)	2.014(6)
Cu(1)–N(4)	2.000(3)	1.971(3)	2.011(6)
Cu(1)–X(1)	2.401(1)	2.515(1)	2.750(1)
N(1)–Cu(1)–N(2)	79.48(10)	80.00(11)	80.3(2)
N(1)–Cu(1)–N(3)	136.03(10)	136.96(11)	138.1(2)
N(1)–Cu(1)–N(4)	99.11(10)	99.18(11)	99.4(2)
N(2)–Cu(1)–N(3)	92.32(11)	92.02(12)	92.2(2)
N(2)–Cu(1)–N(4)	166.67(11)	167.24(12)	168.1(3)
N(3)–Cu(1)–N(4)	79.44(11)	79.85(11)	80.1(2)
X(1)–Cu(1)–N(1)	104.36(8)	104.09(7)	103.77(16)
X(1)–Cu(1)–N(2)	97.18(8)	97.17(9)	96.53(19)
X(1)–Cu(1)–N(3)	119.56(8)	118.90(8)	118.10(16)
X(1)–Cu(1)–N(4)	96.01(8)	95.38(8)	95.10(18)

Results and Discussion

Synthesis

The 1:2 condensation of 1,3-diamidiaminopropane with 2-acetylpyridine produced the neutral tetradentate ligand, N,N′-bis-(1-pyridin-2-yl-ethylidene)-propane-1,3-diamine (*L*), which on reaction with copper(II) perchlorate hexahydrate yielded *[CuL(ClO$_4$)$_2$]*.[30] Reaction of *[CuL(ClO$_4$)$_2$]* with chloride, bromide and iodide separately produced penta-coordinated copper(II) complexes, *[Cu(L)(Cl)]ClO₄* (**1**), *[Cu(L)(Br)]ClO₄* (**2**) and *[Cu(L)(I)]ClO₄* (**3**). The formation of all the complexes is shown in Scheme 1.

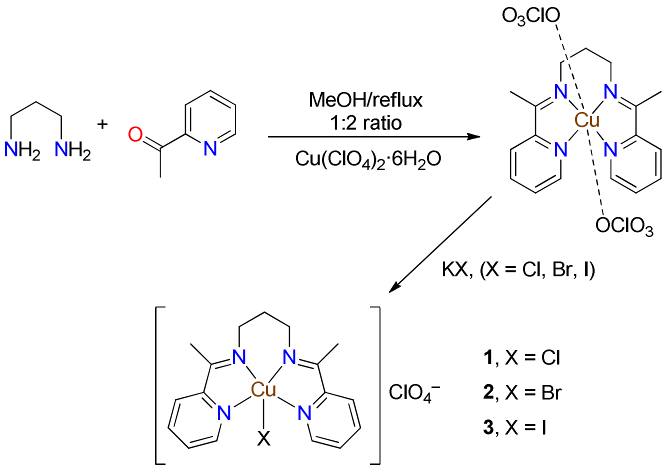

Scheme 1: Synthesis of the complexes **1**-**3**.

IR and UV-VIS spectra, fluorescence, magnetic moments and PXRD

In the IR spectra of all the complexes, no bands due to ν_{NH2} could be observed indicating the condensation of the free amine groups. The bands corresponding to azomethine (C=N) groups are distinct and occur within 1612–1620 cm^{-1}.[40] The lowering of the positions of the bands indicates their coordination to the metal centres. The sharp single peak at about 1088 cm^{-1}foreach of the complexes supports the presence of ionic perchlorate in the complexes.[41] The electronic spectra of all the complexes consist of one d-d transition band of lower intensity in the visible range (~700 nm). Intense bands in the UV region correspond to ligand to metal charge transfer transitions (Fig. 1). All the complexes show luminescence in acetonitrile solution. These are assigned as intra-ligand $^1(\pi\text{–}\pi^*)$ fluorescence. The luminescence data are listed in Table 3 (without solvent correction). The room temperature magnetic susceptibility measurements show that all the complexes have magnetic moments close to 1.73 BM as expected for discrete magnetically non-coupled spin-only value for copper(II) ion, with single unpaired electron sited in an essentially $d_{x^2-y^2}$ orbital. This value was also observed in similar systems.[42-43]

Table 3: Photophysical data for the complexes **1**-**3**.

Complex	Absorption (nm)	Emission (nm)
1	270	301
2	270	301
3	270	301

The experimental PXRD patterns of the bulk products are in good agreement with the simulated XRD patterns from single-crystal X-ray diffraction, indicating consistency of the bulk samples (Figs. S1–S3, Electronic Supplementary Information). The simulated patterns of the complexes are calculated from the single crystal structural data (Cif file) using the CCDC Mercury software.

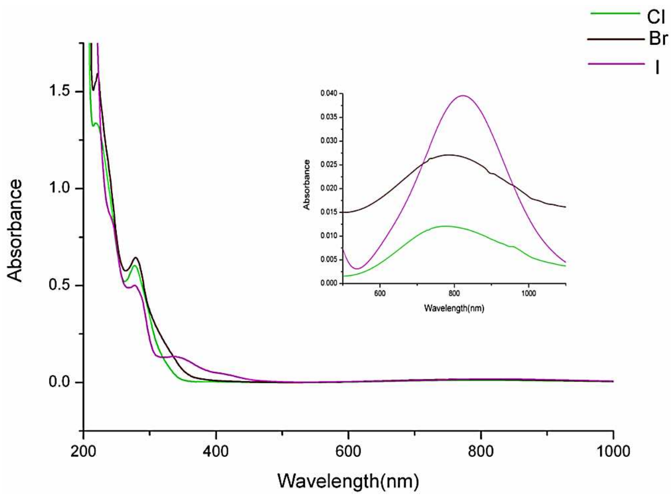

Figure 1: The UV–Vis spectra of the complexes in acetonitrile.

Structure descriptions

Each of the complexes **1-3** crystallises in triclinic space group *P-1*. The structures consist of discrete mononuclear units. The structures of the three complexes are isomorphous. In each of the complexes, the penta-coordinated copper(II) is ligated by two imine nitrogen atoms {N(2), N(3)} and two pyridine nitrogen atoms {N(1), N(4)}, from a tetradentate symmetrical di-Schiff base and a halide co-ligand {Cl(1) in **1**, Br(1) in **2** and I(1) in **3**}. The distortion of the coordination polyhedron from the square pyramid to the trigonal bipyramid is calculated by the Addison parameter (τ) as an index of the degree of trigonality.[44] The value of τ is defined as the difference between the two largest donor-metal-donor angles divided by 60, a value that is 0 for the ideal square pyramid and 1 for the ideal trigonal bipyramid. The Addison parameters are 0.509 (for **1**), 0.503 (for **2**) and 0.497 (for **3**), indicating the actual geometries of copper(II) are intermediate between trigonal bipyramid and square pyramid.

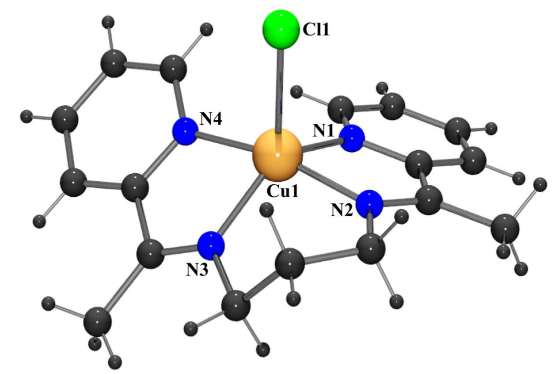

Figure 2: Perspective view of the complex **1**. Only the relevant atoms are labelled. Perchlorate ion is not shown for clarity.

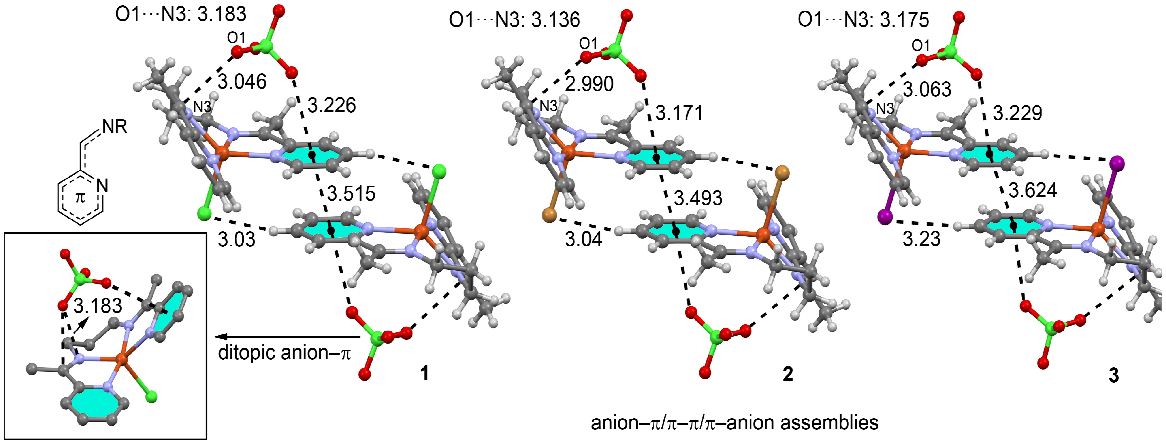

Figure 3: X-ray structure of centrosymmetric compounds **1–3** with indication of the anion/π–π/anion assembly. Non covalent interactions are represented by dashed lines. Distances are in Å.

The perspective view of complex **1** together with the selective atom-numbering scheme is shown in Fig. 2. The molecular structures of complexes **2** and **3** are very similar to that of complex **1**. The perspective views of the complexes **2** and **3** are shown in Figs. S4 and S5 (Electronic Supplementary Information). Deviations of the coordinating atoms, N(1), N(2), N(3) and N(4), from the plane passing through them are 0.256(3), -0.279(3), 0.284(3) and -0.262(3) Å in **1**, 0.256(3), -0.279(3), 0.274(3) and -0.251(3) Å in **2** and 0.251(6), -0.273(7), 0.277(6), -0.254(7) Å in **3**. The copper(II) is displaced 0.4940(4) Å in **1**, 0.4746(4) Å in **2** and 0.4611(9) Å in **3** from this plane towards the coordinated halide. The Cu(1)–halogen bond lengths are 2.4011(11) Å in **1**, 2.5145(8) Å in **2** and 2.7504(11)Å in **3**. In each of the complexes, the six-membered chelate ring, Cu(1)–N(2)–C(8)–C(9)–C(10)–N(3), assumes a boat conformation with puckering parameters, q_3 = -0.055(3) Å, q_2 = Q = 0.757(3) Å, θ = 94.1(2)°, φ = 18.9(3) in **1,** q_3 = -0.069(3) Å, q_2 = Q = 0.755(3) Å, θ = 95.2(2)°, φ = 341.0(3)° in **2** and q_3 = -0.077(8)Å, q_2 = Q = 0.771(8) Å, θ = 95.7(6)°, φ = 18.7(6)° in **3**.[45] The dihedral angle between the pyridine rings of the Schiff base is 55.31(16)° in **1**, 55.70(17)° in **2** and 54.4(4)° in **3**.

Theoretical study

The theoretical study is focused to the analysis of the interesting noncovalent interactions observed in the solid state architecture of the three compounds (Fig. 3) with special interest to the anion/π–π/anion assemblies. All structures are isomorphic and, consequently, they have the same 3D architecture and the distances that characterize each interaction are similar. Obviously, the coordination of the ligand to the Cu(II) ion increases the π-acidity of the ring and the anion–π interaction is expected to be very favorable. In this study we attempt to provide individual energetic values to the different contributions of the noncovalent interactions to the formation of the assembly. In is interesting to note that the anion–π interaction is ditopic; that is the ClO_4^- anion interacts with two different π-systems (considering the C=N double bond as a part of the π-system since it is conjugated with the pyridine ring) by means of two different oxygen atoms (Fig. 3, left).

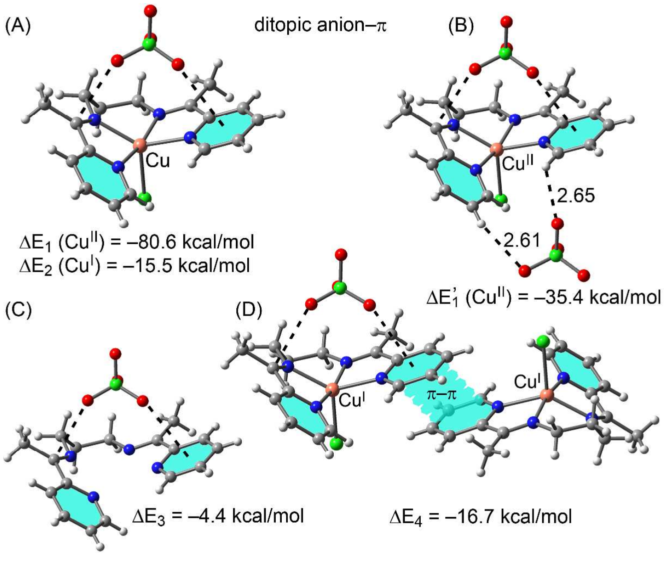

Figure 4: Theoretical models and interaction energies of several anion–π and anion–π–π complexes assemblies based on the solid state structure of compound **1**. Distances are in Å.

We have first analyzed computationally the anion–π interaction using several models (Fig. 4). It should be mentioned that the moiety formed by the Cu(II) metal center complexed to the tetradentate Schiff base ligand and the halide coligand is cationic. Therefore there is a strong contribution of a non directional and purely electrostatic interaction between the counter-ions. In fact the anion–π interaction in compound **1** (selected as a representative model) is ΔE_1 = –80.6 kcal/mol. In order to estimate the strength of the anion–π contact without the contribution of this purely electrostatic interaction, we have used two different theoretical models. In the first one, the Cu(I) metal center has been used instead of Cu(II). As a result the interaction is reduced to ΔE_2 = –15.5 kcal/mol that can be attributed to the double anion–π interaction. In the second one, an additional perclhorate anion has been included in the model (see Figure 4B). In this model the interaction is reduced to $\Delta E_1{}'$ = –35.4 kcal/mol that is considerably more favorable than ΔE_2 (model using Cu(I)) because purely electrostatic interactions are important in this model due to the proximity of the metal ion. Furthermore, we have used another theoretical model where the copper and the halide coligand have been eliminated and only the tetradentate Schiff base ligand and the anion is considered. As a consequence, the interaction is further reduced to a modest ΔE_3 = –4.4 kcal/mol, indicating that the coordination of the ligand to the metal center drastically increases the acidity of the π-system. Finally, we have also study possible cooperativity effects between the anion–π and π–π interactions. In particular we have evaluated the anion–π interaction (using Cu^I) in the theoretical model used shown in Fig. 4D where the π–π interaction has been previously formed and the interaction energy is ΔE_4 = –16.7 kcal/mol (more negative than ΔE_2) indicating that the anion–π interaction is likely reinforced by the presence of the π–π interaction.

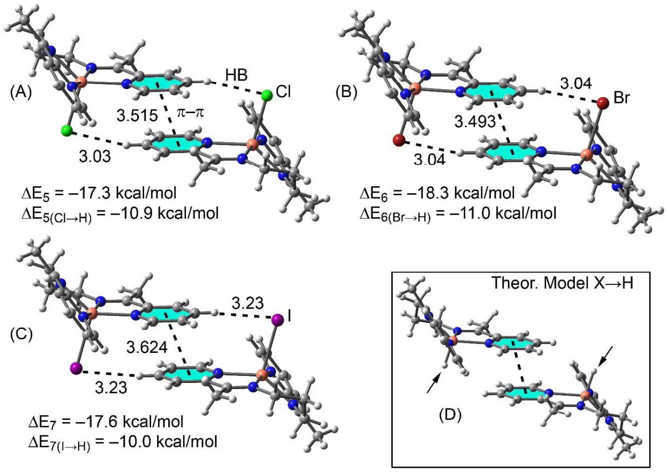

Figure 5: Cu^I-theoretical models and interaction energies of several π–π complexes based on the solid state structure of compound **1–3**. Distances in Å.

We have also analyzed computationally the π–π interaction that is responsible for the formation of the assemblies shown in Fig. 3. In addition to the π-stacking interaction, the complex is further stabilized by two self-complementary C–H···X hydrogen bonds (X = Cl, Br and I, Fig. 5). In order to estimate both interactions separately, we have computed the binding energies of two theoretical models for each compound: one corresponds to the self-assembled dimer found in the X-ray structure and in the other one the halide has been replaced by hydride (highlighted in Fig. 5D). The interaction energies (using Cu^I) for each compound (both models) are summarized in Fig. 5 and from the inspection of the results the following issues arise. First, the π–π interaction is similar in all dimers, ranging from $\Delta E_{7(I\rightarrow H)}$ = –10 kcal/mol to $\Delta E_{6(I\rightarrow H)}$ = –11 kcal/mol. The contribution of both C–H···X hydrogen bonds can be estimated by considering both interaction energies computed for each complex. For instance in compound **1** (X = Cl) the energy associated to each C–H···Cl interaction is ΔE_{HB} = ½[$\Delta E_{7(I\rightarrow H)}$ – ΔE_7] = –3.2 kcal/mol. The H-bonding interaction is similar in all complexes ~3.5 kcal/mol that is modest compared to the anion–π and π–π interactions.

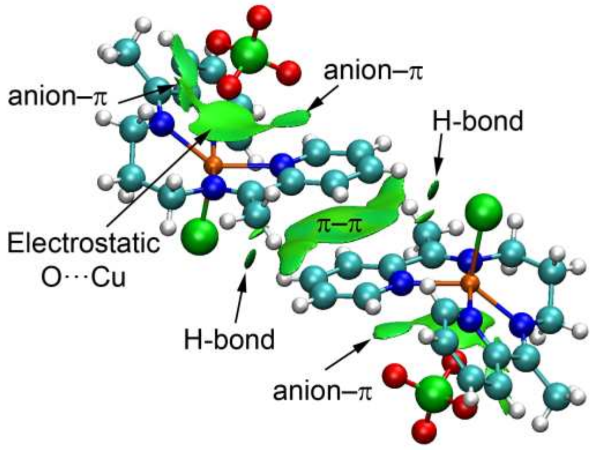

Figure 6: The NCI surface of anion/π–π/anion assembly is shown. NCI surface shows only intermolecular interactions.

Finally, we have used the NCI (Non Covalent Interaction) plot to study the different noncovalent interactions observed in compound **1** as a model of all isomorphic structures. It is a visualization index based on the electron density and its derivatives, and enables identification and visualization of non-covalent interactions efficiently. The isosurfaces correspond to both favorable and unfavorable interactions, as differentiated by the sign of the second density Hessian eigen value and defined by the isosurface color. NCI analysis allows an assessment of host-guest complementarity and the extent to which weak interactions stabilize a complex. In Fig. 6 we show the representation of the NCI plot computed for the anion/π–π/anion assembly. Several non-covalent regions clearly appear between the anions and π-systems. The interaction of the anion with both π-systems of the tetradentate ligand and the Cu atom originates an extended isosurface that almost covers the entire ligand. The π–π interaction is also characterized by an extended isosurface covering both aromatic rings. In contrast the H-bonding interaction is characterized by a very small isosurface that it is a clear indication of the higher directionality of this interaction.

Hirshfeld surfaces

The Hirshfeld surfaces of all the complexes, mapped over a d_{norm} (range of -0.1 to 1.5 Å), shape index and curvedness are illustrated in Figures 7-9. The surfaces are shown as transparent to allow visualization of the molecular moiety, in a similar orientation for both structures, around which they are calculated.

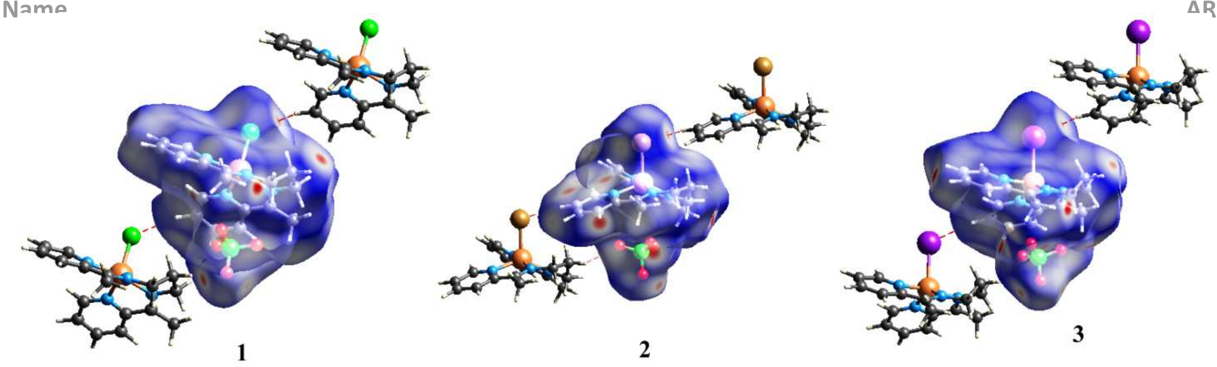

Figure 7: Hirshfeld surfaces mapped over d_{norm} for complexes **1** (left), **2** (middle) and **3** (right).

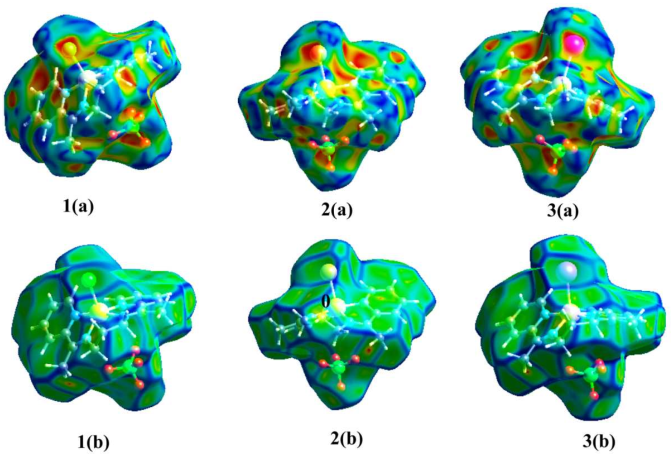

Figure 8: Hirshfeld surfaces mapped over shape index (top) and curvedness (bottom) for complexes **1** (left), **2** (middle) and **3** (right).

The dominant interaction between halogen (X) and hydrogen (H) atoms can be observed in the Hirshfeld surface as the red areas in Figure 7. Other visible spots in the Hirshfeld surfaces correspond to O···H and H···H contacts. The small extent of area and light color on the surface indicates weaker and longer contact other than hydrogen bonds. The X···H/H···X intermolecular interactions appear as distinct spikes in the 2D fingerprint plots (Figure 9). Complementary regions are visible in the fingerprint plots where one molecule act as donor (de>di) and the other as an acceptor (de<di). The fingerprint plots can be decomposed to highlight particular atoms pair close contacts. This decomposition enables separation of contributions from different interaction types, which overlap in the full fingerprint. The proportions of X···H/H···X interactions comprise 13.6%, 14.0% and 13.3% of the Hirshfeld surfaces for each molecule of the complexes **1**, **2** and **3** respectively. The X···H interaction is represented by a spike (di=1.667, de= 1.053 Å in **1**, di=1.76, de=1.033 Å in **2** and di=1.866, de=1.047 Å in **3**) in the bottom left (donor) area of the fingerprint plot (Figure 9). The H···X interaction is also represented by another spike (de=1.667, di=1.067 Å in **1**, de=1.753, di=1.033 Å in **2** and de=1.866, di=1.04 Å in **3**) in the bottom right (acceptor) region of fingerprint plot and can be viewed as a pair of large red spots on the d_{norm} surface (Figure 7).

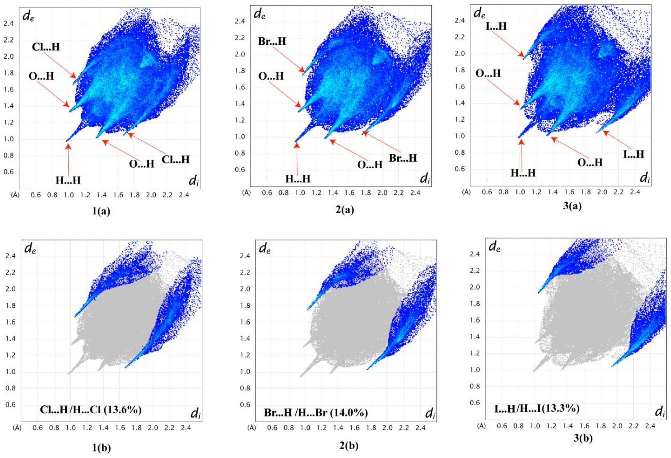

Figure 9: Fingerprint plots of **1** (left), **2** (middle) and **3** (right): Full (top) and resolved into X···H/H···X (bottom) contacts showing the percentages of contacts contributed to the total Hirshfeld Surface area of molecules [X= Cl in **1**, Br in **2** and I in **3**].

Conclusion

We have synthesized three mononuclear copper(II) complexes with a tetradentate Schiff base, halide co-ligands and perchlorate as counter anion (**1-3**). A common feature in all compounds is the formation of anion/π–π/anion assembly that is crucial to explain the 3D architecture of the complexes in the solid state. In the theoretical study we have estimated the contribution of each interaction to the formation of the assembly and the interplay between the anion–π and π–π interactions. The mutual reinforcement of both interactions has been demonstrated computationally. The assignment of the contribution of each interaction and its mutual influence is certainly important to gain general knowledge in the intricate mechanism that governs the molecular recognition and crystal packing since it could be useful to the crystal engineering community. It was found that the systematic change of the halide co-ligands in compounds **1**–**3** has a very small influence upon the interaction energies of both the π–π and C–H···X hydrogen bonds that are responsible for the formation of the self-assemblies in their solid state structures. Finally, the NCI plot reveals extended surfaces that characterize the less directional aromatic interactions and a small surface characterizing the more directional C–H···X hydrogen bonds.

Hirshfeld surfaces were also drawn to support the C–H···X hydrogen bonds.

Acknowledgments

This work was supported by the CSIR, India (Sanction number. 01(2730)/13/EMR-II dated 18.04.2013), the DGICYT of Spain (projects CTQ2011-27512/BQU and CONSOLIDER INGENIO 2010 CSD2010-00065, FEDER funds) and the Direcció General de Recercai Innovació del Govern Balear (project 23/2011, FEDER funds). We thank the CTI (UIB) for free allocation of computer time. P.P.J wishes to thank VR, the Swedish Research Council for the financial support. A.B. thanks the UGC, India, for awarding a Junior Research Fellowship.

Notes and references

[a]Department of Chemistry, Inorganic Section, Jadavpur University, Kolkata -700032, India.
e-mail: shouvik.chem@gmail.com, Tel: +(91)33-2457-2941
[b]Departament de Química, Universitat de les Illes Balears, Crta. de Valldemossa km 7.5, 07122 Palma (Baleares), Spain.
[c]CAS Chemical Centre, Lund University, Getingevägen 60, Box 124, Lund SE-22100, Sweden.
[d]School of Chemistry, The University of Reading, P.O. Box 224, Whiteknights, Reading RG6 6AD, United Kingdom.

† Electronic Supplementary Information (ESI) available: CCDC 975407, 975408 and 975409 contain the supplementary crystallographic data for 1, 2 and 3 respectively. These data can be obtained free of charge via http://www.ccdc.cam.ac.uk/conts/retrieving.html or from the Cambridge Crystallographic Data Centre, 12 Union Road, Cambridge CB2 1EZ, UK; fax: (+44) 1223-336-033; or e-mail: deposit@ccdc.cam.ac.uk. See DOI: 10.1039/b000000x/

1 (a) H. J. Schneider, *Angew. Chem. Int. Ed*., 2009, **48**, 3924–3977; (b) J. -M. Lehn, *Supramolecular Chemistry*; VCH: Weinheim, Germany, 1995; (c) J. W. Steed and J. L. Atwood, *Supramolecular Chemistry*; Wiley: Chichester, U.K., 2000.

2 (a) G. R. Desiraju, *Acc. Chem. Res*., 2002, **35**, 565–573; (b) G. R. Desiraju, *Nature,* 2001, **412**, 397–400; (c) H. M. Lee, S. B. Suh, J. Y. Lee, P. Tarakeshwar and K. S. Kim, *J. Chem. Phys*., 2000, **112**, 9759–9772; (d) B. H. Hong, J. Y. Lee, C.-W. Lee, J. C. Kim, S. C. Bae and K. S. Kim, *J. Am. Chem. Soc*., 2001, **123,** 10748–10749; (e) T. Steiner, *Angew. Chem. Int. Ed*., 2002, **41,** 48–76.

3 (a) C. A. Hunter and J. K. M. Sanders, *J. Am. Chem. Soc*., 1990, **112**, 5525−5534; (b) S. K. Burley and G. A. Petsko, *Science,* 1985, **229**, 23−28; (c) K. S. Kim, P. Tarakeshwar and J. Y. Lee, *Chem. Rev*., 2000, **100,** 4145−4185.

4 (a) J. C. Ma and D. A. Dougherty, *Chem. Rev*., 1997, **97**, 1303−1324; (b) K. S. Kim, J. Y. Lee, S. J. Lee, T.-K. Ha and D. H. Kim, *J. Am. Chem. Soc*., 1994, **116**, 7399−7400.

5 (a) M. Nishio, M. Hirota and Y. Umezawa, *In The C−H/π Interaction: Evidence, Nature, Consequences*; Wiley-VCH: New York, 1998; (b) M. Nishio, *CrystEngComm.,* 2004, **6**, 130−156.

6 (a) M. Egli and S. Sarkhel, *Acc. Chem. Res*., 2007, **40**, 197−205; (b) T. J. Mooibroek, P. Gamez and J. Reedijk, *CrystEngComm.,* 2008, **10**, 1501−1515; (c) J. Ran and P. Hobza, *J. Chem. Theory Comput*., 2009, **5**, 1180−1185; (d) M. Barceló-Oliver, C. Estarellas, A. García-Raso, A. Terrón, A. Frontera, D. Quiñonero, E. Molins and P. M. Deyà, *CrystEngComm.,* 2010, **12,** 362−365.

7 D. Quiñonero, C. Garau, C. Rotger, A. Frontera, P. Ballester, A. Costa and P. M. Deyà, *Angew. Chem. Int. Ed*., 2002, **41,** 3389−3392.

8 (a) A. Frontera, F. Saczewski, M. Gdaniec, E. Dziemidowicz-Borys, A. Kurland, P. M. Deyà, D. Quiñonero and C. Garau, *Chem. Eur. J*., 2005, **11,** 6560−6567; (b) M. Mascal, *Angew. Chem. Int. Ed*., 2006, **45,** 2890−2893; (c) G. Gil-Ramirez, E. C. Escudero-Adan, J. Benet-Buchholz and P. Ballester, *Angew. Chem. Int. Ed*., 2008, **47**, 4114−4118; (d) B. L. Schottel, H. T. Chifotides and K. R. Dunbar, *Chem. Soc. Rev*., 2008, **37,** 68−83; (e) P. Gamez, T. J. Mooibroek, S. J. Teat and J. Reedijk, *Acc. Chem. Res*., 2007, **40**, 435−444; (f) A. Perez-Velasco, V. Gorteau and S. Matile, *Angew. Chem. Int. Ed*., 2008, **47**, 9603−9607; (g) R. E. Dawson, A. Hennig, D. P. Weimann, D. Emeryl, V. Ravikumar, J. Montenegro, T. Takeuchil, S. Gabutti, M. Mayor, J. Mareda, C. A. Schalley and S. Matile, *Nat. Chem*., 2010, **2**, 533−538.

9 (a) V. Gorteau, G. Bollot, J. Mareda, A. Perez-Velasco and S. Matile, *J. Am. Chem. Soc*., 2006, **128**, 14788–14789; (b) V. Gorteau, G. Bollot, J. Mareda and S. Matile, *Org. Biomol. Chem*., 2007, **5**, 3000–3012.

10 (a) Y. Zhao, N. Sakai and S. Matile, *Nature Commun*., 2014, **5**, 3911. (b) Y. Zhao, N. Sakai and S. Matile, *Angew. Chem. Int. Ed*., 2013, **52,** 9940–9943. (c) Y. Zhao, N. Sakai and S. Matile, *J. Am. Chem. Soc*., 2014, **136**, 2101–2111. (d) A. Bauza, D. Quinonero, P. M. Deya and A. Frontera, *Chem. Eur. J*., 2014, **20**, 6985–6990. (e) A. Bauza, D. Quinonero, P. M. Deya and A. Frontera, *Chem. Asian J*., 2013, **8**, 2708–2713.

11 M. Mascal, A. Armstrong and M. D. Bartberger, *J. Am. Chem. Soc*., 2002, **124,** 6274−6276.

12 (a) B. L. Schottel, H. T. Chifotides and K. R. Dunbar, *Chem. Soc. Rev*., 2008, **37**, 68−83; (b) B. P. Hay and V. S. Bryantsev, *Chem. Commun*., 2008, 2417−2428; (c) A. Frontera, P. Gamez, M. Mascal, T. J. Mooibroek and J. Reedijk, *Angew. Chem., Int. Ed.* 2011, **50**, 9564−9583; (d) A. Frontera, *Coord. Chem. Rev*., 2013, **257**, 1716–1727.

13 O. B. Berryman, F. Hof, M. J. Hynes and D. W. Johnson, *Chem. Commun*., 2006, 506−508.

14 I. Alkorta, I. Rozas and J. Elguero, *J. Am. Chem. Soc*., 2002, **124,** 8593−8598.

15 (a) D. Kim, E. C. Lee, K. S. Kim and P. Tarakeshwar, *J. Phys. Chem. A*, 2007, **111**, 7980−7986; (b) B. Han, J. J. Lu and J. K. Kochi, *Cryst. Growth Des*., 2008, **8**, 1327−1334; (c) C. Estarellas, M. C. Rotger, M. Capo, D. Quinonero, A. Frontera, A. Costa and P. M. Deya, *Org. Lett*., 2009, **11**, 1987−1990.

16 (a) R. Biswas, C. Diaz, A. Bauzá, A. Frontera and A. Ghosh, *Dalton Trans.,* 2013, **42**, 12274-12283; (b) R. Biswas, C. Diaz, A. Bauzá, M. B. -Oliver, A. Frontera and A. Ghosh, *Dalton Trans.,* 2014, **43** 6455-6467; (c) S. Chattopadhyay, M. G. B. Drew, C. Diaz and A. Ghosh, *Dalton Trans.,* 2007, 2492-2494; (d) P. Bhowmik, H. P. Nayek, M. Corbella, N. Aliaga-Alcalde and S. Chattopadhyay, *Dalton Trans.*, 2011, **40**, 7916-7926; (e) L. K. Das, A. Biswas, J. S. Kinyon, N. S. Dalal, H. Zhou and A. Ghosh, *Inorg. Chem.,* 2013, **52**, 11744-11757; (f) P. Seth, A. Bauzá, A. Frontera, C. Massera, P. Gamez and A. Ghosh, *CrystEngComm.,* 2013, **15**, 3031–3039; (g) L. K. Das and A. Ghosh, *CrystEngComm.,* 20134, **15**, 9444–9456; (h) L. K. Das, A. M.

Kirillov and A. Ghosh, *CrystEngComm.,* 2014, **16**, 3029–3039; (i) D. Rehder, Inorg. *Chem. Commun.,* 2013, **6**, 604–617; (j) X. Li, M. S. Lah and V. L. Pecoraro, *Inorg. Chem.,* 1988, **27**, 4664-4668; (k) L. Casella and M. Gullotti, *J. Am. Chem. Soc.,* 1981, **103**, 6338-6347.

17 (a) S. Bag, P. K. Bhaumik, S. Jana, M. Das, P. Bhowmik and S. Chattopadhyay, *Polyhedron,* 2013, **65**, 229–237; (b) P. K. Bhaumik, K. Harms and S. Chattopadhyay, *Polyhedron,* 2013, **62**, 179–187; (c) M. Das and S. Chattopadhyay, *Polyhedron,* 2013, **50**, 443–451; (d) P. Bhowmik, S. Chatterjee and S. Chattopadhyay, *Polyhedron,* 2013, **63**, 214–22;. (e) S. Jana, P. Bhowmik, M. Das, P. P. Jana, K. Harms and S. Chattopadhyay, *Polyhedron,* 2012, **37,** 21–26.

18 (a) N. Brĕfuel, I. Vang, S. Shova, F. Dahan, J. –P. Costes and J. –P. Tuchagues, *Polyhedron,* 2007, **26**, 1745–175; (b) T. K. Karmakar, G. Aromŕ, B. K. Ghosh, A. Usman, H. –K. Fun, T. Mallah, U. Behrens, X. Solans and S. K. Chandra, *J. Mater. Chem.,* 2006, **16**, 278–285; (c) T. K. Karmakar, B. K. Ghosh, A. Usman, H. –K. Fun, E. Riviĕre, T. Mallah, G. Aromŕ and S. K. Chandra, *Inorg. Chem.*, 2005, **44**, 2391-2399; (d) P. S. Mukherjee, S. Dalai, E. Zangrando, F. Lloret and N. R. Chaudhuri, *Chem. Commun*., 2001, 1444–1445; (e) M. Habib, T. K. Karmakar, G. Aromŕ, J. R. -Arińo, H. –K. Fun, S. Chantrapromma and S. K. Chandra, *Inorg. Chem*., 2008, **47**, 4109-4117.

19 (a) Q. Lu, C. -Y. Shen and Q. -H. Luo, *Polyhedron*, 1993, **12**, 2005-2008; (b) Q. -H. Luo, Q. Lu, A. -B. Dai and L. -R. Huang, *Inorg. Biochem.,* 1993, **51**, 655-662.

20 (a) M. Linss and U. Weser, *Inorg. Chim. Acta*, 1986, **125**, 117-121; (b) C. -M. Liu, R. -G. Xiong, X. -Z. You, Y. -J. Liu and K. -K. Cheung, *Polyhedron*, 1996, **15**, 4565-4571; (c) J. Müller, K. Felix, C. Maichle, E. Lengfelder, J. Strähle and U. Weser, *Inorg. Chim. Acta*, 1995, **233**, 11-19; (d) P. A. Cerutti, Science, 1985, **277**, 375-381.

21 (a) L. –J. Liu, *Acta Cryst*., 2011, **E67**, m876; (b) L. –J. Liu, *Acta Cryst*., 2011, **E67**, m878; (c) B. Samanta, J. Chakraborty, C. R. Chowdhury, S. K. Dey, D. K. Day, S. R. Batten, P. Jensen, G. P. A. Yap and S. Mitra, *Struct. Chem*., 2007, **18,** 33-41; (d) C. -M. Liu, R. -G. Xiong, X. -Z. You, H. -K. Fun and K. Sivakumar, *Polyhedron*, 1997, **16**, 119-123.

22 S. Chattopadhyay, M. G. B. Drew and A. Ghosh, *Inorg. Chim. Acta*, 2006, **359**, 4519-4525.

23 O. Kahn, *Molecular magnetism*; VCH, New York, 1993.

24 G. M. Sheldrick, *SHELXS-97 and SHELXL-97, Program for Structure Solution*, University of Gottingen, Germany, 1997.

25 A. L. Spek, *Acta Cryst.*, 1990, **A46** C34.

26 K. Diamond, *Crystal Impact GbR*, Bonn, Germany, 2007.

27 M. N. Burnett and C. K. Johnson*, ORTEP-3: Oak Ridge Thermal Ellipsoid Plot Program for Crystal Structure Illustrations*, Report ORNL-6895, Oak Ridge National Laboratory, Oak Ridge, TN, USA, 1996.

28 C. F. Macrae, I. J. Bruno, J. A. Chisholm, P. R. Edgington, P. McCabe, E. Pidcock, L. R. Monge, R. Taylor, J. van de Streek and P. A. Wood, *J. Appl. Crystallogr.*, 2008, **41**, 466-470.

29 R. Ahlrichs, M. Bär, M. Hacer, H. Horn and C. Kömel, *Chem. Phys. Lett.*, 1989, **162**, 165–169.

30 S. Grimme, J. Antony, S. Ehrlich, and H. Krieg, *J. Chem. Phys.*, 2010, 1**32**, 154104-154119.

31 (a) E. Johnson, S. Keinan, P. Mori-Sánchez, J. Contreras-García, A. Cohen and W. Yang, *J. Am. Chem. Soc*., 2010, **132**, 6498–6506; (b) J. Contreras-García, E. Johnson, S. Keinan, R. Chaudret, J. Piquemal, D. Beratan and W. Yang, *J. Chem. Theory Comput.*, 2011, **7**, 625–632; (c) J. Contreras-García, W. Yang and E. Johnson, *J. Phys. Chem. A*, 2011, **115**, 12983–12990.

32 M. A. Spackman and D. Jayatilaka, *CrystEngComm.,* 2009, **11**, 19-32.

33 F. L. Hirshfeld, *Theor. Chim. Acta*, 1977, **44**, 129-138.

34 H. F. Clausen, M. S. Chevallier, M. A. Spackman and B. B. Iversen, *New J. Chem.,* 2010, **34**, 193-199.

35 A. L. Rohl, M. Moret, W. Kaminsky, K. Claborn, J. J. McKinnon and B. Kahr, *Cryst. Growth Des.*, 2008, **8**, 4517-4525;

36 A. Parkin, G. Barr, W. Dong, C. J. Gilmore, D. Jayatilaka, J. J. McKinnon, M. A. Spackman and C. C. Wilson, *CrystEngComm.,* 2007, **9**, 648-652;

37 M. A. Spackman and J. J. McKinnon, *CrystEngComm.,* 2002, **4**, 378-392.

38 S. K. Wolff, D. J. Grimwood, J. J. McKinnon, D. Jayatilaka and M. A. Spackman, *Crystal Explorer 2.0*, University of Western Australia: Perth, Australia, 2007; http://hirshfeldsurfacenet.blogspot.com

39 J. J. McKinnon, M. A. Spackman and A. S. Mitchell, *Acta Cryst.*, 2004, **B60**, 627–668.

40 S. Chattopadhyay, M. S. Ray, S. Chaudhuri, G. Mukhopadhyay, G. Bocelli, A. Cantoni and A Ghosh, *Inorg. Chim. Acta,* 2006, **359**, 1367-1375.

41 S. Jana, P. Bhowmik, M. Das, P. P. Jana, K. Harms and S. Chattopadhyay, *Polyhedron*, 2012, **37**, 21–26.

42 M. S. Ray, R. Bhattacharya, S. Chaudhuri, L. Right, G. Boceli, G. Mukhopadhyay and A. Ghosh, *Polyhedron*, 2003, **22**, 617-624.

43 M. Liang, W. Z. Wang, Z. Q. Liu, D. Z. Liao, Z. H. Jiang, S. P. Yan and P. Cheng, *J. Coord. Chem*., 2003, **56**, 1473-1480.

44 A. W. Addison, T. N. Rao, J. Reedjik, J. van Rinj and C. G. Verscholar, *J. Chem. Soc., Dalton Trans.*, 1984, 1349-1356.

45 (a) D. Cremer and J. A. Pople, *J. Am. Chem. Soc.*, 1975, **97**, 1354-1358; (b) D. Cremer, *Acta Cryst.*, 1984, **B40**, 498-500; (c) J. C. A. Boeyens, *J. Cryst. Mol. Struct.*, 1978, **8**, 317-320.